Photoacoustic radar imaging signal-to-noise ratio, contrast, and resolution enhancement using nonlinear chirp modulation

Bahman Lashkari and Andreas Mandelis*

Center for Advanced Diffusion-Wave Technologies, Department of Mechanical and Industrial Engineering, University of Toronto, Toronto, M5S 3G8, Canada
**Corresponding author: mandelis@mie.utoronto.ca*

Received October 9, 2009; revised March 25, 2010; accepted April 19, 2010; posted April 19, 2010 (Doc. ID 118397); published May 6, 2010

Cross-correlation (radar) frequency-domain photoacoustic (PA) imaging parameters [signal-to-noise ratio (SNR), contrast, and spatial resolution] are explored. The application of nonlinear frequency modulation instead of the standard linear frequency chirps is investigated. In addition to the image produced by the amplitude of the cross correlation between input and detected signals, the phase of the correlation signal is used as a filter of the PA amplitude combined with linear or nonlinear frequency chirps to improve SNR, contrast, and spatial resolution. The experimental results with a high-frequency transducer exhibit more than 10 and 8 times contrast enhancement using nonlinear and linear chirps, respectively. Concomitant improvements in SNR and image resolution were also observed. © 2010 Optical Society of America

OCIS codes: 110.5120, 110.5125.

Photoacoustic (PA) imaging can be implemented either in time domain by powerful nanosecond laser pulses or in frequency domain (FD) by low-power intensity-modulated cw laser irradiation. In our previous work [1] FD-PA imaging with linear frequency-swept optical modulation was implemented, and the application of various signal processing methods to obtain depth-selective imaging was demonstrated. Very recently [2] we compared the FD and pulsed techniques with respect to the maximum detectable depth using a dual-mode PA system. The present study investigates the application of the FD technique using its major controllable aspects: frequency bandwidth and signal spectral distribution.

In the FD technique, to determine the depths of chromophores, matched-filter compression [1,3] can be used; the cross correlation of the detected acoustic signal, $s(t)$, and the incident laser waveform, $r(t)$, are calculated, and the delay time of the peak represents the subsurface position of a chromophore. Matched-filter compression can give the highest signal-to-noise ratio (SNR) for an input signal buried in white noise [3]. Since the PA system incorporates the effect of its own impulse response in the output, the matched filter cannot be obtained exactly; therefore the SNR of the filter will degrade with respect to the matched filter. The PA system also induces a phase change in the generated acoustic transient. Hence, in addition to in-phase cross correlation, the cross correlation of the detected signal with the quadrature of the input waveform is also available. By combining the in-phase and quadrature cross correlations, the envelope cross correlation will be obtained. The resulting envelope signal benefits from the total energy imparted and detected and therefore provides higher SNR than does in-phase correlation alone. Furthermore, it provides a smoother trace compared to its components, which relaxes the requirement for extra frequency-domain windowing used in our previous work [1]. Nevertheless, time tapering of the amplitude of the input waveform proved to increase the SNR owing to elimination of the Fresnel ripples [4].

Figure 1 describes the signal generation pathway in frequency domain using the fast Fourier transform module. The quadrature of the input waveform is calculated by Hilbert transformation; Z^* and IFFT blocks represent the complex conjugate and inverse fast Fourier transform, respectively. The calculation of the in-phase and quadrature cross correlations yields additional significant information that is the phase of the detected transient with respect to the input waveform. This phase depends on optical and acoustic properties of the medium and the characteristics of the ultrasonic transducer. Despite the fact that the evaluation of these parameters individually is impractical, the value of the correlation phase should remain unchanged for a fixed position of the specimen–transducer distance and in the absence of noise. Therefore, if the experiment is repeated by using a continuous sequence of chirps at each coordinate point, the standard deviation (SD) of the phase can be used as an indicator of the presence of a signal-producing chromophore; small SD values express statistical fluctuation in a real signal, and large values reveal noise.

The first experiment demonstrates the effects of bandwidth and nonlinearity on the achieved SNR in the FD method. The instrumentation and experimental setup employed in this study are described elsewhere [2]. A train of 1 ms intensity-modulated 1064 nm laser chirps illuminated a tissue phantom,

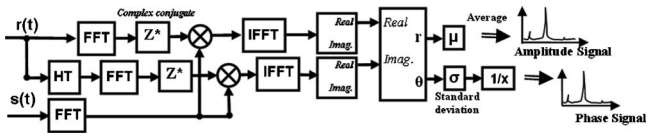

Fig. 1. Schematic signal-processing technique for the FD method.

0146-9592/10/101623-3/$15.00

and the induced acoustic waves were detected by a 3.5 MHz ultrasonic transducer (Panametrics V382 with −6 dB range of 2.66 to 5.23 MHz). The phantom was made of PVC plastisol with an inclusion placed 6 mm below the surface. The absorption- and reduced-scattering coefficients of the surrounding plastisol were 0.2 and 3.1 cm^{-1}, respectively, and the absorption coefficient of the inclusion was 4 cm^{-1}. Figure 2(a) shows the amplitudes of the cross-correlation signals generated with linear frequency modulation (LFM) using three different bandwidths of 1–3 MHz, 0.5–3 MHz, and 0.5–5 MHz. The peaks flagged A in the figures are from PA signals generated on the surface of the phantom, and the major peaks marked B are the response of the inclusion. Despite the lower photon flux to which the inclusion is exposed compared with the phantom surface, B-peaks are stronger than A-peaks because of their higher absorption coefficient of the inclusion than the surroundings. The SNRs are indicated in the insets. Theoretically the SNR enhancement is equal to the time-bandwidth product [3]; therefore the maximum available transducer bandwidth is expected to generate the best SNR. Our experimental results demonstrate that the maximum SNR is achieved by the 0.5–3 MHz bandwidth. This can be explained by considering that the PA efficiency will decrease and acoustic attenuation will increase with frequency. Therefore for PA phenomena an optimal bandwidth exists that depends on the physical properties of the media.

Figure 2(b) demonstrates the application of nonlinear chirps within the same bandwidths. This experiment is designed to evaluate the possibility of benefiting from the maximum available bandwidth while concentrating more on the optimal frequency range. The chirps are

$$r(t) = \cos\left(2\pi f_0 t + \frac{2\pi B}{n T_{ch}^{n-1}} t^n\right), \quad (1)$$

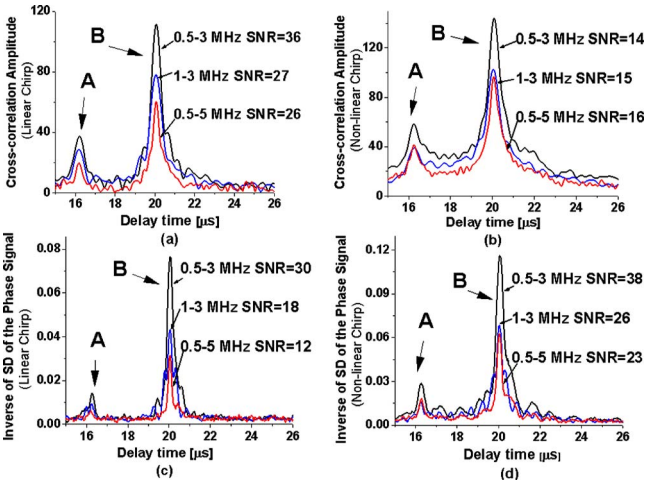

Fig. 2. (Color online) Effect of bandwidth and nonlinearity on SNR. Cross-correlation amplitude generated by (a) linear and (b) nonlinear chirps. Inverse of the SD of the phase generated by (c) linear and (d) nonlinear chirps.

where f_0, B, and T_{ch} are initial frequency, frequency bandwidth, and chirp duration, respectively. Parameter n is 2 for linear chirps and 2.5 for the employed nonlinear chirps. The area under the correlation curve corresponds to the total output energy of the filter with constant input energy; it was thus demonstrated that the specified nonlinear chirps can increase the generated PA energy (magnitude of cross-correlation amplitude). However, these chirps also generate bigger sidelobes and broaden the peak of the envelope correlation, thereby degrading the SNR. Thus, similar to pure modulated ultrasound imaging, LFM provides the best SNR [4].

Figures 2(c) and 2(d) demonstrate the inverse of the SD of the phase signals generated in the same experiments. Again the same bandwidth of 0.5 to 3 MHz provides the best SNR, which is reasonable, because the stronger the amplitude, the more stable the phase values will be. However, unlike amplitude, in the phase signal the nonlinear chirps provide higher SNR than the linear chirps, which can be explained by considering that the phase signal is less broadened than the amplitude signal and therefore does not contribute to noise floor as amplitude does in the nonlinear case.

Figure 3 demonstrates that the nonlinear chirp SNR improvement property in the phase signal can be combined with the linear chirp amplitude signal to enhance the contrast of the combined image. It compares three images of a 6.4 mm diameter cylindrical inclusion located 13.7 mm below the surface perpendicular to the plane of the image. The optical properties of the inclusion and the surroundings were similar to the previous experiment. Figure 3(a) is the image generated by correlation amplitude with linear chirp (0.5–3 MHz bandwidth). Figures 3(b) and 3(c) depict the amplitude image multiplied by linear and nonlinear phase signals, respectively. A broadened line and part of a curvature are visible in the images, which are, respectively, related to the top surface of the phantom and the cylindrical inclusion. Since the inclusion was located very deep inside the medium, a linear time gain correction (TGC) was applied to the signals, or the phantom surface signal would dwarf the inclusion signal. In all images, because of TGC, more speckle noise is observable below the inclusion than above it. To compare the contrast of the images, we use the following contrast measure suggested by Patterson and Foster [5]:

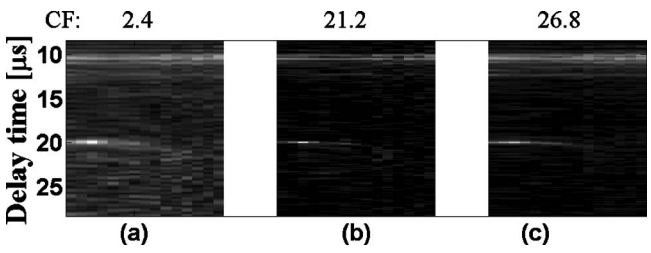

Fig. 3. Images generated by (a) amplitude signal, (b) amplitude signal filtered by phase signal (linear chirp), and (c) amplitude signal filtered by phase signal (nonlinear chirp), with a high-frequency transducer (3.5 MHz).

$$\mathrm{CF} = \frac{\text{Signal mean in the lesion} - \text{mean in the background}}{\text{Signal mean in the background}}. \quad (2)$$

The evaluated contrast factors (CFs) are 2.4, 21.2, and 26.8 for Figs. 3(a)–3(c), respectively. This shows that by using the phase signal obtained from a nonlinear chirp, we enhanced the contrast of the amplitude and resolution of the image [see Fig. 4(b)] more than 10 times. This is 26% higher than the amplitude image filtered by the phase image obtained with a linear chirp. Another experiment was undertaken to compare the contrast between pulsed and FD methods employing a 500 kHz center frequency transducer (Panametrics V391). The inclusion was PVC plastisol with absorption coefficient 2 cm^{-1} positioned at the fixed focal distance with respect to the transducer in deep intralipid solution [2]. The laser wavelength for both methods was the same (1064 nm), and the imparted energies were 7.13 mJ/cm^2 per chirp and 15.5 mJ/cm^2 per pulse. 800 chirps and 60 pulses were utilized to generate each signal trace. The repetition frequency of the pulsed laser was 10 Hz, and 800 chirps consisted of 16 trains of fifty 1 ms chirps with around 1 s break time between them, which was required for the software to process the collected data. To comply with safety limits for the cw case, the energy imparted in 50 ms (50 consecutive chirps) should be less than 2.6 J/cm^2, and the average power should be less than 1 W/cm^2. For pulsed laser the maximum permissible exposure (MPE) is 100 mJ/cm^2 per pulse [6]. Measurements in this Letter did not exceed these upper limits. The signal traces in each part of Fig. 4, from top to bottom, correspond to 20 to 28 mm overlayers of intralipid solution (0.47%), with the intralipid thickness increasing by 2 mm steps. Figure 4(a) shows the cross-correlation amplitude traces generated by the FD method using a linear chirp. Figure 4(b) is the signal traces generated by filtering the amplitude signal using the SD of the correlation phase by multiplying those signals (linear chirp). This operation enhances the SNR and contrast and narrows the peak FWHM, thus greatly enhancing spatial resolution despite the use of a low-frequency transducer. Figure 4(c) shows the PA responses to the pulsed laser. The CFs of all signal traces are shown beside them to assist the comparison.

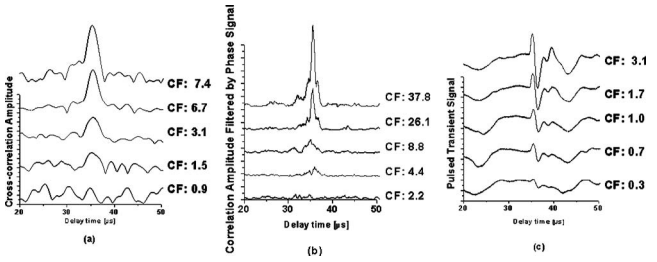

Fig. 4. Comparison of signal traces produced with (a) FD amplitude, (b) combined FD amplitude and phase, and (c) pulsed-laser method, using a low-frequency transducer (500 kHz).

These experiments with the 500 kHz transducer demonstrated two notable differences with the high-frequency transducer: nonlinear chirps cannot generate a significant increase in the SNR of the phase signal, and the optimal frequency bandwidth is the maximum available bandwidth (200–800 kHz). To explain these effects, the one-dimensional solution of the PA pressure field [2] has shown that the maximum pressure occurs at an angular frequency equal to the product of the chromophore absorption coefficient and the speed of sound, around 100 kHz for the used phantoms. For the 500 kHz transducer, this frequency range is located near the peak of its transfer function, and thus any extra weighting of the frequency-sweep rate is not beneficial. That is not the case for the 3.5 MHz transducer, where the frequency range is far from the optimal frequency.

In summary, it was demonstrated that the optimal bandwidth for a PA system is not determined exclusively by the transducer bandwidth but can be strongly affected by the physical properties of the interrogated material. The inverse of the standard deviation of the correlation phase was shown to provide an additional imaging channel comparable to the amplitude channel. The phase-filtered PA amplitude image exhibited an increase of more than 1 order of magnitude in contrast to the nonfiltered cross-correlation amplitude and the pulsed-laser PA method. Nonlinear phase filtering also enhanced spatial resolution by a factor of about 2.6 through peak narrowing.

A. Mandelis gratefully acknowledges the support of the Canada Foundation for Innovation (CFI), the Ontario Research Fund (ORF), and the Canada Research Chairs (CRC). The authors further acknowledge the NSERC Discovery Grants program and the MRI Ontario Premier's 2007 Discovery Award in Science and Engineering to A. M.

References

1. S. A. Telenkov, A. Mandelis, B. Lashkari, and M. Forcht, J. Appl. Phys. **105**, 102029 (2009).
2. S. A. Telenkov and A. Mandelis, J. Biomed. Opt. **14**, 044025 (2009).
3. C. E. Cook and M. Bernfeld, *Radar Signals: an Introduction to Theory and Application* (Artech House, 1993).
4. T. Misaridis and J. A. Jensen, IEEE Trans. Ultrason. Ferroelectr. Freq. Control **52**, 192 (2005).
5. M. S. Patterson and F. S. Foster, Ultrason. Imaging **5**, 195 (1983).
6. American National Standards Institute, American National Standard for the Safe Use of Lasers in Health Care Facilities: Standard Z136.1-1993 (ANSI, Inc., 1993).